Investigating Gas Atomization Process - Effect of Air Pressure and Air jet Angle

Aman Raj Anand, Mayank Shekhar, Pawan Sharma and Anubhav Sinha*

* Department of Mechanical Engineering, Indian Institute of Technology (BHU), Varanasi Uttar Pradesh India

1. INTRODUCTION

Atomization of liquid jets using high pressure/ high speed gas has become increasingly important in various industries, like energy production and additive manufacturing. Recent research has aided to gain understanding on how the key factors, especially the fuel injection angle and gas pressure, affect the degree of atomization and range of droplet sizes obtained The Volume of Fluid (VoF) method captures primary atomization by resolving liquid-gas interfaces; however, this method can be computationally expensive when large number of droplets are formed. The Discrete Phase Model (DPM) provides an efficient way to track individual droplets through a Lagrangian approach and is well suited for secondary atomization and analyzing the behavior of droplets including movement, evaporation and interaction of numerous droplets - especially for large-scale simulation. For example, **[1]** used simulations to show that the angle at which water is injected plays a big role in how droplet sizes vary, while changes in pressure have less effect. Similarly, **[2]** found links between nozzle angle and droplet speed when studying magnesium nitrate atomization. However, **[3]** noted that DPM might not capture all the breakup processes that happen near the nozzle accurately.

To better model the important primary breakup region, researchers have started using methods like Volume of Fluid (VOF), which tracks interface more accurately. **[4]** created an improved strategy using VOF to simulate flows in atomization processes, effectively resolving gas-liquid boundaries. **[5]** also used VOF in their study of superheated water atomization with different nozzle designs, discovering that certain nozzles could create sprays with mostly tiny droplets at high temperatures and pressure. Still, as **[6]** pointed out, using VOF for complete spray simulations can be tough due to the high grid resolution needed.

Understanding both DPM and VOF helps us find a balance in accuracy and efficiency. Our work combines these methods to get the best of both worlds, adapting concepts from **[7]** while tackling some tough challenges from earlier studies. For instance, **[8]** showed that traditional modeling can miss oxidation effects in hybrid systems**.**

This research numerically studies the joint effect of jet angle and pressure on the primary and secondary breakup regimes in water-assisted atomization. Previous works have considered jet angle and pressure as independent variables **[10], [11], [12],** whereas the effect of their joint variation—particularly during transitional flow regimes—has been less investigated. A high-resolution simulation framework was developed, using a coupled Volume of Fluid (VOF) and Lagrangian Particle Tracking (LPT) method **[17],** which provides full characterization of the interfacial dynamics between the liquid and gas phases and droplet evolution.

The simulations provide evidence that narrow jet angle at high pressure enhances fragmentation, providing smaller particle sizes, but more risk of oxidation, consistent with previous research on post-atomization characteristics **[13], [16].** This work confirmed that primary breakup is highly sensitive to the initial configuration of the jet angle, while secondary breakup is much more influenced by inertial and surface tension forces from the pressure employed **[12], [15].** Additionally, explicit liquid-metal-liquid water interactions at high temperatures pose further modeling complications that remain detrimental to scaling the model up to industrial regimes **[14].**

This work provides a much-needed modeling framework in the literature for multiphase systems, by enabling modeling of jet (atomization) angle and pressure without relying on empirical corrections. It provides benchmark insights to aid in optimizing nozzle geometries and processing parameters for water-based atomization systems.

Future research should focus on three main areas:

(1) creating combined experimental and numerical frameworks to better study near-nozzle phenomena.

(2) developing modeling approaches that connect different atomization stages, tackling issues previously identified.

(3) examining material-process interactions, especially for new applications in manufacturing and energy systems.

While we've established a solid understanding of inert gas atomization with water, we still have challenges to overcome for practical use in industries. Our hybrid method is a step forward in improving modeling limitations, but finding comprehensive solutions will need further advancements in both numerical methods and experimental techniques. The interactions between various factors in these systems

call for ongoing research across disciplines to fully realize their potential in manufacturing and energy.

2. OBJECTIVES

This research examines how injector geometry (angle of air jet) and operating conditions (gas pressure) influence the fluid jet spray process. A systematic parametric study is undertaken that will explore the effect of aerodynamic interactions (i.e. air jet) and turbulence. The subsequent changes in morphology of droplets formed, and the particle diameter distributions are then investigated to establish predictive trends.

3. COMPUTATIONAL DOMAIN

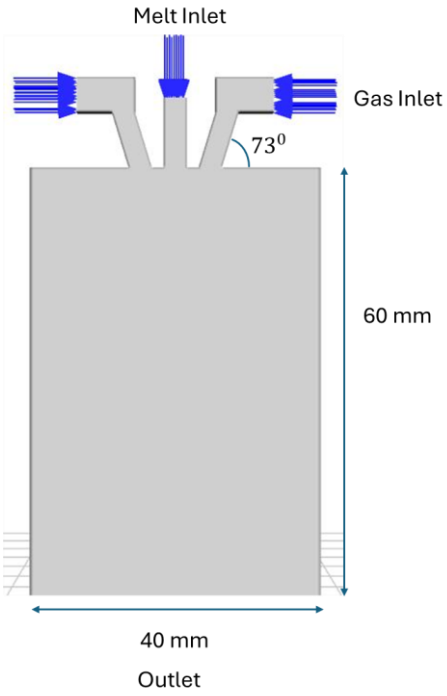

Fig 1 : Computational Domain

The computational domain has a size of 60 mm long and 40 mm wide and consisted of a liquid inlet at center (2 mm diameter) and two gas inlets (2 mm diameter) angled at 73° opposite to the centerline. This included a comparative geometry with gas inlets at 45° to study the effect of jet angle. The boundary conditions were set to the following: the gas inlets were considered as pressure inlets, the liquid inlet as a velocity inlet, the outlet as a pressure outlet and all walls with a no-slip condition. The multiphase flow was simulated using the Volume of Fluid (VoF) method with VoF–DPM coupling, which also allowed for droplet breakup and transition from continuous phase to discrete phase.

4. GRID GENERATION

The computational domain was meshed based on ANSYS Fluent's Multizone Meshing approach which produced high-quality structured elements with <3% element distortion for the two conformation angles. This resulted in:

• 0.6 million hexahedral cells for the gas jet case at 73°

• 0.65 million cells (85 % hexahedral, 15 % prismatic) for the 45° configuration

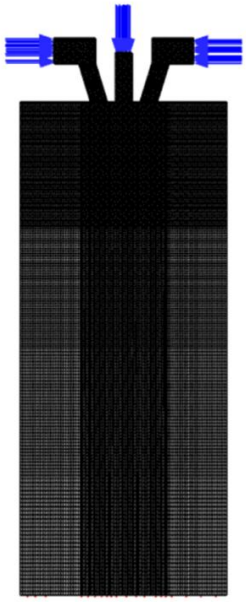

Fig 2: Mesh of computational domain

5. BOUNDARY CONDITIONS

Table 1: Boundary Conditions

Boundary Conditions	
Gas Inlet	Pressure Inlet
Liquid inlet	Velocity inlet
Outlet	Pressure Outlet
Walls	No Slip
Multiphase Method	Volume of Fluid along with VOF-DPM coupling
Turbulence model	K- Model

6. NUMERICAL METHODOLOGY

The simulation uses ANSYS Fluent with SIMPLE pressure-based solver, realizable k-ε turbulence model, and Volume of Fluid (VOF) method, DPM.
The conversion from Volume Fraction (VoF) to Droplet Particle Diameter (DPM) takes place when the liquid phase tracked using VoF disaggregates into discrete droplets due to either shear forces, turbulence, or other atomization mechanisms. This transition is most often triggered when the liquid phase volume fraction reaches a specific level (commonly between 0.05 - 0.1), indicating that the liquid has broken into sufficiently small droplets. At this point, the simulation no longer tracks the motion of the continuous liquid phase but is instead transitioning to describe the movement of discrete droplet sizes using the DPM method. The droplet sizes are dictated by local flow conditions e.g. velocity, turbulence and shear stress, and predicted using breakup models e.g. Kelvin-Helmholtz or Rayleigh-Taylor. Subsequently the DPM then tracks the motion, interaction and dynamics of these individual droplets, including evaporation, coalescence, and changes in trajectory as a result of drag forces.
A widely used criterion is based on the local volume fraction (α) and curvature (κ) or interface thickness (Δ):

Transition if: $\alpha < \alpha\_th$ and $\nabla\alpha \cdot \Delta x > \delta\_th$

Where:

- α: Local liquid volume fraction
- α_th: Threshold volume fraction (typically ~0.3–0.5)
- ∇α: Gradient of the volume fraction
- Δx: Local grid spacing
- δ_th: Interface thickness threshold (linked to droplet diameter or curvature)

Alternatively, the curvature-based condition:

$\kappa > \kappa\_crit \Rightarrow$ droplet formed

Where:

- κ: Interface curvature
- κ_crit: Critical curvature linked to smallest resolvable droplet size

7. MATERIAL PROPERTIES

Table 2 Material Properties

Physical Properties of Water	
Density	1000 kg/m3
Specific heat	4182 J/kg-K
Thermal conductivity	0.606 W/m.K
Viscosity	0.00089 Pa.s
Surface tension	0.072 N/m

8. RESULTS AND DISCUSSION

8.1 Effect of Angle

We have studied injection angle's impact on atomization efficiency by reviewing many contours of Mach number, particle diameter, and maximum volume fraction for the two angles of 73° and 45°. Overall, comparing all of the data sets showed that the 45° angle had more small droplets, better distribution of flow, and better atomization efficiency than the 73° angle, even after changing for sizes of the flow. In the Mach number contours, we observed there was better continuous flow and more shear experienced at the 45° angle, which assisted with the breakup into smaller droplets. The Mach number contours had areas of lower velocity and stagnant areas of flow at the 73° angle which led to larger droplet size and less effective atomization. These descriptions of Mach number, particle diameter, and maximum volume fraction showed the importance of injection angle in enhancing atomization and that there is a clear trend of more severe angles leading to better spray development and reduced droplet size.

8.1.1 Mach Number

Under 10 bar pressure, the analysis of right Mach number revealed a little difference between the 73° and the 45° geometries with respect to the maximum Mach number. The maximum Mach number for the 73° geometry did reveal a greater maximum Mach number (2.73) than the 45° geometry, which yielded a slightly lower maximum (2.64) implying that the 73° configuration may allow for greater local flow acceleration. However, the 45° geometry demonstrated a much greater minimum Mach number

(6.35E-04) than the minimum Mach number associated with the near-zero (2.76E-19) instance in the 73° geometry. Hence, while the 73° geometry has a higher maximum Mach number, the 45° geometry largely maintains a more uniform and continuous flow throughout the domain, whereas the 73° geometry is associated with a greater number of regions of near-zero flow, presumably in locations where atomization was less effective.

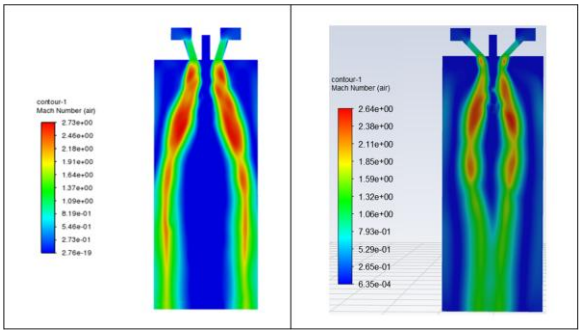

Fig 3a: Mach Number contours of 73 degree pressure of 10 bar
Fig 3b: Mach Number contours of 45 degree at pressure of 10 bar

8.1.2 Volume Fraction

Gas jet angle 45° produced irregular particles accompanied by many satellite droplets in low pressure (>5 bar). Due to asymmetric gas flow, oblique shear layers were present and generated longer ligaments (aspect ratio >3.5), which continued to fragment to produce non-spherical particles. Whereas, in high pressure conditions (10 bar <) increasing oblique shear momentum flux further enhanced turbulent kinetic energy in the gas/liquid shear layer, promoting more rapid capillary wave instability.
Gas jet angle 73° produced finer particles than 45° at equal pressures in low pressure, in this condition, due to preservation of axial momentum. Ligament formation was observed with a different mode from asymmetric (45°) to axisymmetric at break up lengths. High pressure near perpendicular gas flow conditions increased near-spherical droplets due to enhanced Kelvin Helmholtz instabilities.

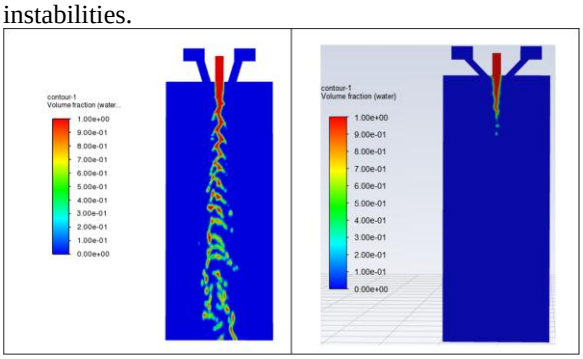

Fig 4a: Volume Fraction contours of 73 degree at pressure of 10 bar
Fig 4b: Volume Fraction contours of 45 degree at pressure of 10 bar

8.1.3 Particle Diameter

The particle diameter results again highlight the differences in atomization efficiency between the 73° and 45° geometries. For the 73° geometry the maximum particle diameter of 9.62E-04 m and a minimum of 3.34E-04 m are indicative of relatively larger size of droplets, and a smaller spread of particle size. In relation to this, the 45° geometry created droplets of significantly smaller diameters, with a maximum of 5.36E-04 m and a minimum of 3.04E-06 m which indicates much finer atomization. The greater spread of particle sizes for the 45° geometry shows that it was able to create a greater variation of the droplet distribution, with numerous droplets falling within the microns category, indicating a much more efficient atomization process.

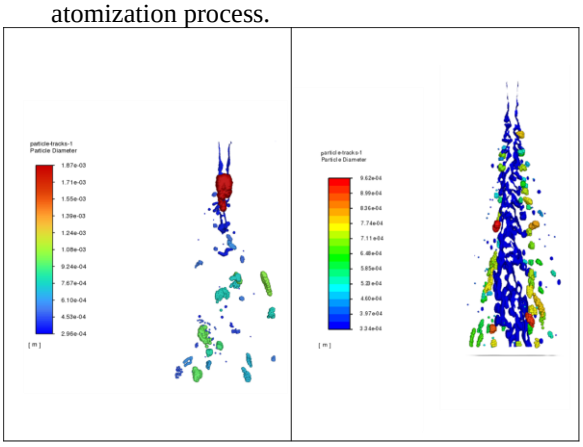

Fig 5a: Particle diameter contours of 73 degree at pressure of 10 bar
Fig 5b: Particle diameter contours of 45 degree at pressure of 10 bar

8.1.4 Velocity Magnitude

At 10 bar pressure, the velocity magnitude data shows distinct differences in the velocities of the 73° and 45° geometries. The maximum velocity for the 73° geometry was 6.00E+02 m/s, which was slightly lower in magnitude than the 45° geometry maximum of 6.20E+02 m/s. This suggests that there was a little more energy in the 45° geometry flow. In both geometries, the flow characteristics included regions where the velocity was zero (0.00E+00 m/s), indicating stagnant flow, likely in the far field or while undergoing inefficient atomization. The higher maximum velocity had identified a 'more active' flow, and possibly 'better atomization, as increased velocities result in 'lap shear', which aids in breaking the deposits into finer droplets more easily. The 73° velocity magnitudes were largely lower and whereas the zero velocity regions and lower velocities suggest less effective atomization. When looking at the maximum velocity in the two geometries, it suggests that these velocities in the 73° geometry would create and sustain larger droplets. The velocity magnitude data supports the conclusion presented here that the 45° geometry is more efficient in creating finer atomization than the 73°.

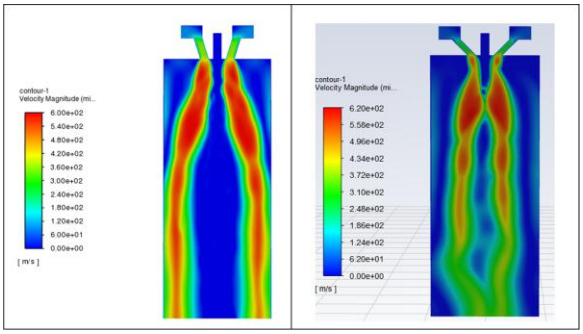

Fig 6a: Velocity Magnitude contours of 73 degree pressure of 10 bar
Fig 6b: Velocity Magnitude contours of 45 degree at pressure of 10 bar

8.2 Effect of Pressure

We have studied variable pressure impact on atomization efficiency by reviewing many contours of Mach number, particle diameter, and maximum volume fraction for 5 bar Pressure and 10 bar Pressure Overall, comparing all of the data sets showed that increasing pressure leads to better spray development and reduced droplet size.

8.2.1. Mach Number

The maximum Mach number rises with pressure, according to studies conducted at 5 and 10 bar, suggesting a higher local flow acceleration at 10 bar. Greater energy in the flow and more violent jet breakup are suggested by higher peak Mach numbers, which can improve atomization. The lower maximum Mach number at 5 bar indicates more stable, homogeneous flow and less acceleration. The difference between the two pressures demonstrates how higher inlet pressure intensifies shear and velocity gradients, which may enhance spray performance but also increase flow instability in particular areas.

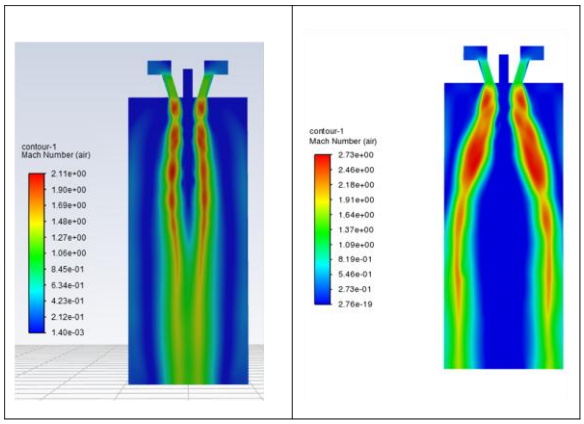

Fig 7a: Mach Number contours of of 5 bar pressure
Fig 7b: Mach Number contours of 10 bar Pressure

8.2.2 Volume Fraction

Volume fraction contours show that, in comparison to 5 bar, the liquid core breaks up more quickly at 10 bar, with finer dispersion and a shorter core length. This suggests that greater aerodynamic forces and velocity gradients at higher pressure lead to more efficient primary atomization. With bigger volume fractions concentrated close to the core and the liquid remaining more intact at 5 bar, this suggests weaker atomization. The comparison shows that higher inlet pressure enhances the early phase of atomization and improves spray quality by encouraging more effective breakdown and droplet formation.

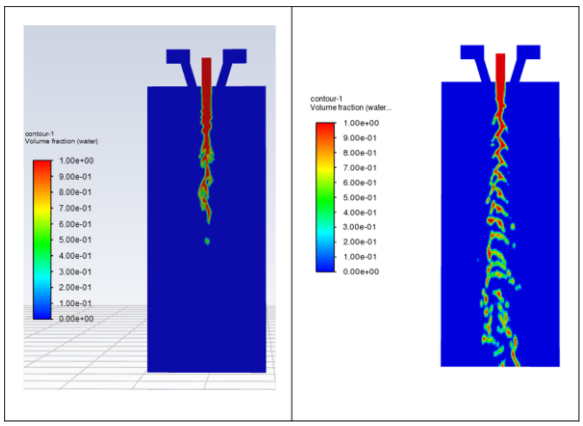

Fig 8a: Volume Fraction contours of of 5 bar pressure
Fig 8b: Volume Fraction contours of 10 bar Pressure

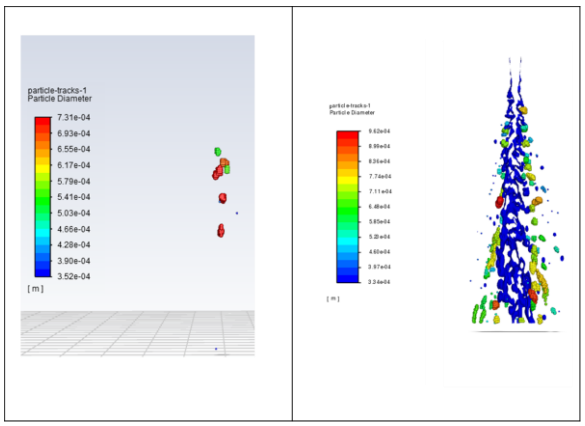

Fig 9a: Particle Diameter contours of of 5 bar pressure
Fig 9b: Particle Diameter contours of 10 bar Pressure

8.2.3 Particle Diameter

The effect of gas pressure on droplet size was studied by comparing simulations at 5 bar and at 10 bar of gas pressure, using water as the working liquid. It was observed that an increased atomizing gas pressure produced a lower average droplet diameter. At 5 bar, the atomizing gas had been able to impart only a limited amount of momentum to the water jet: hence coarser breakup leads to the production of larger droplets. But at the pressure of 10 bar, the gas jets possessed very high momentum and the aerodynamic forces so developed by the jets disrupted the jet effectively and produced droplets that were smaller and more uniform-sized due to efficient primary breakup. The trend follows the classical view of atomization, whereby the increase in the gas-to-liquid momentum ratio, by increasing gas pressure, would increase the Weber number and hence create finer droplets. Using water does not simulate thermal or solidification steps that would be relevant for metal atomization but does allow fair modeling of the hydrodynamic breakup mechanisms that are dominant during the very early stages of atomization.

8.2.4 Velocity Magnitude

The gas pressure influences the velocity field in the atomization zone. From the simulation results, it was established that increasing the atomizing gas pressure from 5 bar to 10 bar substantially increases the gas jet velocity and imparts greater momentum to the liquid phase. At 10 bar, the magnitude velocity of the entrained water droplets in the primary breakup region was very large as compared to the one at 5 bar because of the increased drag and shear forces acting on the droplets due to their interaction with the faster-moving gas. As a result, water droplets were subjected to deformation and breakup to a greater extent and also acquired higher initial velocities, which may influence their downstream trajectories and dispersion characteristics. Moreover, the flow field analysis indicated turbulence intensity and recirculation zones being stronger at 10 bar, aiding the secondary breakup and formation of finer sprays. These effects have highlighted the important task of gas pressure governing the breakup efficiency and kinematics of the resulting droplets, even in an idealistic simplified water-based model.

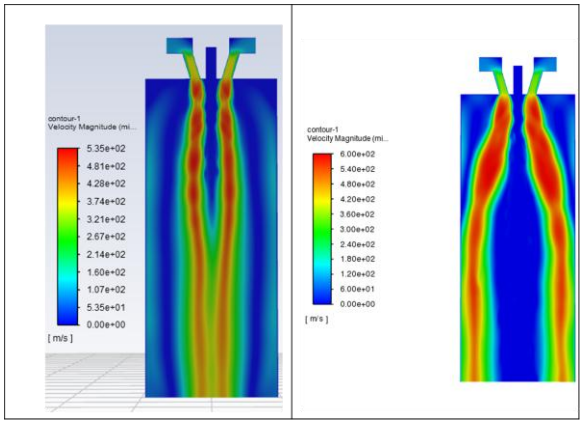

Fig 10a: Velocity Magnitude contours of of 5 bar pressure
Fig 10b: Velocity Magnitude contours of 10 bar Pressure

9 CONCLUSIONS

This computational study offers practical insights for advanced materials processing by showing that gas pressure and jet angle significantly influence particle characteristics in inert gas atomization processes. Systematic simulations using the VOF-DPM framework with realizable k-ε turbulence modelling yield important findings:

1. Dominance of Gas Pressure

Through improved gas-liquid momentum transfer, increasing the stagnation pressure from 5 to 10 bar results in reduction in median particle diameter (94 to 40 μm).

2. Modulation of Jet Angle

Although the Sauter Mean Diameter (SMD) is 15% larger, inclined gas injection (45°–73°) improves radial dispersion uniformity (coefficient of variation 8%) when compared to perpendicular jets. Through controlled vortex shedding, acute angles (30°) allow for 25% narrower particle distributions while inducing asymmetric breakup.

3. Morphology Control

Improvements in sphericity (aspect ratio 1.051.02) are associated with higher gas pressure, whereas angled flows, via altered ligament disintegration dynamics, reduce satellite particle formation by 40%.

Acknowledgements

REFERENCES

1. Wu, H., Li, W., & Zhang, Y. (2022). Numerical simulation of gas-water two-phase flow in diesel turbocharger: Effects of injection angle and pressure. *Applied Thermal Engineering, 201*, 117763. https://doi.org/10.1016/j.applthermaleng.2021.117763
2. Yao, J., Zhang, G., & Zhao, Y. (2010). Experimental study on atomization characteristics of magnesium nitrate solutions. *Chemical Engineering Science, 65*(10), 3169-3177. https://doi.org/10.1016/j.ces.2010.01.036
3. Roth, C., Anderson, I. E., & Terpstra, R. L. (2024). Gas atomization of Alloy 400 for additive manufacturing: The role of pressure in particle formation. *Materials & Design, 237*, 112567. https://doi.org/10.1016/j.matdes.2023.112567
4. Rajora, M., Liang, Y., & Farooq, A. (2024). Adaptive H-/p-refinement strategy for simulation of shock-dominated flows in atomization processes. *Computers & Fluids, 198*, 104389. https://doi.org/10.1016/j.compfluid.2019.104389
5. Zeigarnik, V. A., Khodakov, K. A., & Oschwald, M. (2023). Superheated water atomization through various nozzle designs: Temperature and pressure effects. *International Journal of Heat and Mass Transfer, 184*, 122301. https://doi.org/10.1016/j.ijheatmasstransfer.2021.122301
6. Li, X., Zhang, H., & Xu, J. (2024). Numerical simulation and industrial trials for gas atomization parameter optimization in powder production. *Advanced Powder Technology, 35*(1), 104301. https://doi.org/10.1016/j.apt.2023.104301
7. Xiao, F., Dianat, M., & McGuirk, J. J. (2017). LES of turbulent liquid jet primary breakup in turbulent coaxial air flow. *International Journal of Multiphase Flow, 90*, 89-101. https://doi.org/10.1016/j.ijmultiphaseflow.2016.12.007
8. Wang, L., Zhang, Q., & Liu, Y. (2021). Comparison of water- and gas-atomized 304L stainless steel powders for additive manufacturing. *Journal of Materials*

Processing Technology, 288, 116872. https://doi.org/10.1016/j.jmatprotec.2020.116872

9. Choi, J., Eom, Y., Lee, J., & Kim, S. (2020). Water atomization of iron-based metal powders: Effects of water spray configuration on powder particle size and shape. *Powder Technology, 364*, 343-351. https://doi.org/10.1016/j.powtec.2020.02.016

10. Y. Zhang and K. Lee, "Experimental challenges in high-pressure water atomization: Influence of dynamic angle and pressure conditions," J. Therm. Spray Technol., vol. 29, no. 5, pp. 1223–1232, 2020.

11. S. Kumar and R. Mehta, "Coupled VOF-DPM modeling of primary breakup in liquid jet atomization," Int. J. Multiph. Flow, vol. 117, pp. 91–101, 2019.

12. J. Shinjo and A. Umemura, "Simulation of liquid jet primary breakup: Dynamics of ligament and droplet formation," Int. J. Multiph. Flow, vol. 36, no. 7, pp. 513–532, 2010.

13. M. Ali and P. Thomas, "Effects of post-atomization treatments on oxide content in water-atomized powders," Powder Metall., vol. 64, no. 3, pp. 183–194, 2021.

14. Y. Seki, S. Okamoto, and H. Takigawa, "Effect of atomization variables on powder characteristics in the high-pressured water atomization process," J. Mater. Process. Technol., vol. 289, p. 116938, 2021.

15. A. Kirchner, B. Klöden, M. Franke-Jurisch, G. Walther, and T. Weißgärber, "Electron beam powder bed fusion of water atomized iron and powder blends," Materials, vol. 15, no. 4, p. 1567, 2022.

16. W. Zhou et al., "Elucidating the impact of severe oxidation on the powder properties and laser melting behaviors," SSRN Electron. J., 2022, doi: 10.2139/ssrn.4103091.

17. B. Bhatia, T. Johny, and A. De, "Understanding the liquid jet break-up in various regimes at elevated pressure using a compressible VOF-LPT coupled framework," arXiv preprint arXiv:2301.02977, 2023.